Cancer Cell
Article

Chronic Pancreatitis Is Essential for Induction of Pancreatic Ductal Adenocarcinoma by K-Ras Oncogenes in Adult Mice

Carmen Guerra,[1,*] Alberto J. Schuhmacher,[1] Marta Cañamero,[2] Paul J. Grippo,[3] Lena Verdaguer,[1] Lucía Pérez-Gallego,[2,6] Pierre Dubus,[4] Eric P. Sandgren,[5] and Mariano Barbacid[1,*]
[1] Molecular Oncology Program
[2] Biotechnology Program
Centro Nacional de Investigaciones Oncológicas, E-28029 Madrid, Spain
[3] Department of Surgery, Feinberg School of Medicine, Northwestern University, Chicago, IL 60611, USA
[4] EA2406 University of Bordeaux 2, F-33076 Bordeaux, France
[5] Department of Pathobiological Sciences, School of Veterinary Medicine, University of Wisconsin-Madison, Madison, WI 53706, USA
[6] Present address: Anatomical Pathology Service, Hospital General de Palencia "Río Carrión," E-34008 Palencia, Spain
*Correspondence: mcguerra@cnio.es (C.G.), mbarbacid@cnio.es (M.B.)
DOI 10.1016/j.ccr.2007.01.012

SUMMARY

Pancreatic ductal adenocarcinoma (PDA), one of the deadliest human cancers, often involves somatic activation of K-*Ras* oncogenes. We report that selective expression of an endogenous K-*Ras*^{G12V} oncogene in embryonic cells of acinar/centroacinar lineage results in pancreatic intraepithelial neoplasias (PanINs) and invasive PDA, suggesting that PDA originates by differentiation of acinar/centroacinar cells or their precursors into ductal-like cells. Surprisingly, adult mice become refractory to K-*Ras*^{G12V}-induced PanINs and PDA. However, if these mice are challenged with a mild form of chronic pancreatitis, they develop the full spectrum of PanINs and invasive PDA. These observations suggest that, during adulthood, PDA stems from a combination of genetic (e.g., somatic K-*Ras* mutations) and nongenetic (e.g., tissue damage) events.

INTRODUCTION

Pancreatic ductal adenocarcinoma (PDA) is one of the most deadly human tumors, with less than a 3% 5 year survival rate. Painstaking histological, genetic, and clinical studies have identified three different ductal preneoplastic lesions as potential precursors of PDA. They include intraductal papillary mucinous neoplasms (IPMNs) that arise in the main pancreatic duct or its major branches, pancreatic intraepithelial neoplasias (PanINs) that originate within intralobular ducts, and mucinous cystic neoplasms (MCN) that are mucin-producing epithelial neoplasms with a characteristic ovarian-type stroma. All of these preneoplastic lesions are likely to represent progressive stages of the disease (Hruban et al., 2000; Maitra et al., 2005).

Among these preneoplastic lesions, PanINs are the best characterized at the anatomopathological and molecular levels (Hruban et al., 2005). For instance, PanINs progress through well-defined stages (PanIN1A/B to PanIN3) that display increased architectural and cytological atypia. Moreover, each of these PanINs has been associated with specific genetic changes (Hruban et al., 2005). For instance, about 40% of human PanIN1A/B contain mutations in K-*Ras* (review in Tuveson and Hingorani,

SIGNIFICANCE

Human PanINs and PDA have been faithfully reproduced in mouse models by expressing an endogenous K-*Ras* oncogene in pancreatic lineages during embryonic development. Here, we describe a mouse model that allows controlled temporal expression of an endogenous K-*Ras*^{G12V} oncogene in cells of acinar and centroacinar origin. These mice develop the full spectrum of PanINs and invasive PDA when K-*Ras*^{G12V} expression is allowed during embryonic development. Surprisingly, K-*Ras*^{G12V} expression in adult mice does not result in neoplastic development unless they undergo chronic pancreatitis. Previous epidemiological studies have identified pancreatitis as a risk factor for human PDA. Thus, close monitoring of people who may have suffered pancreatic tissue damage may help to identify PDA patients in the early stages of the disease.

2005), an oncogene present in most (80%–90%) PDAs (Almoguera et al., 1988). These early lesions also overexpress the HER2 receptor. Increased histological changes are associated with inactivation or loss of the P16INK4a tumor suppressor (55% in PanIN2). Finally, high-grade PanIN3 often display inactivation of P53, loss of SMAD4, and loss of BRCA2 with various frequencies (Tuveson and Hingorani, 2005). These genetic alterations are also found in PDA, thus supporting the concept that PanINs are precursors of the invasive tumors (Hruban et al., 2000, 2005).

Considerable efforts have been made during the last decade to generate animal models that faithfully recapitulate the natural history of human PDA. Most models involve expression of K-*Ras* oncogenes (Aguirre et al., 2003; Brembeck et al., 2003; Grippo et al., 2003; Hingorani et al., 2003; Quaife et al., 1987; Tuveson et al., 2006), although transgenic expression of other oncogenes such as polyoma middle T and growth-promoting molecules, including Shh, HB-EGF, and TGFα, have also been utilized (Hruban et al., 2006). More recently, the PTEN tumor suppressor has been conditionally deleted in early pancreatic progenitors (Stanger et al., 2005). Yet, only the model of Hingorani and coworkers recapitulates the full spectrum of PanIN lesions most commonly identified in PDA patients (Hingorani et al., 2003). In this model, an endogenous K-*Ras*^{G12D} oncogene (Jackson et al., 2001) is turned on during the early stages of embryonic pancreatic development by expressing a Cre recombinase under the control of the *Pdx1* or *P48* promoters (Kawaguchi et al., 2002; Kim and MacDonald, 2002). Thus, in this model, expression of the endogenous K-*Ras*^{G12D} oncogene occurs in all pancreatic lineages since early (E8.5) embryonic development (Hingorani et al., 2003).

Studies aimed at defining the pancreatic lineage responsible for PDA development have not provided conclusive information. Surprisingly, expression of oncogenic K-*Ras* transgenes in ductal lineages under the control of the *Cytokeratin* 19 promoter has failed to induce PanINs or PDA (Brembeck et al., 2003). These observations suggest that PDA originates either from early precursors before they are committed to ductal lineages or by transdifferentiation of other pancreatic cell types. The latter hypothesis has been explored by expressing K-*Ras* oncogenes in cells of acinar lineage under the control of the *Elastase* promoter. Although some of these mice occasionally display low-grade PanINs (P.J.G., unpublished data), they do not develop high-grade lesions or PDA (Grippo et al., 2003). More recently, knockin of a K-*Ras* oncogene in the locus encoding Mist1, a transcription factor required for proper acinar organization, induces invasive and metastatic pancreatic tumors (Tuveson et al., 2006). Yet, these tumors display mixed histological characteristics that do not recapitulate the basic properties of human PDA.

In this study, we have crossed our previously described conditional K-*Ras*^{LSLG12Vgeo} knocked in mice (Guerra et al., 2003) with a bitransgenic strain that expresses the Cre recombinase under the control of the rat *Elastase* promoter using a tet-off strategy (P.J.G. and E.P.S., unpublished data). We report that restricted expression of this endogenous K-*Ras*^{G12V} oncogene in acinar/centroacinar cells results in a full range of PanINs and PDA histologically indistinguishable from those of human patients (Hruban et al., 2006). Moreover, this model allows temporal control of K-*Ras* oncogene expression. Unexpectedly, turning on K-*Ras*^{G12V} in adult acinar cells fails to induce PanINs and PDA. However, if these adult mice undergo chronic pancreatitis, they develop the full spectrum of PanINs and invasive PDA. These observations raise the possibility that human PDA may require, in addition to somatic activation of K-*Ras* oncogenes, nongenetic events involving tissue damage and/or an inflammatory response.

RESULTS

Inducible Expression of an Endogenous K-*Ras*^{G12V} Oncogene in Pancreatic Acinar and Centroacinar Cells

To express an endogenous K-*Ras*^{G12V} oncogene in pancreatic cells of acinar lineage, we crossed our conditional K-*Ras*$^{+/LSLG12Vgeo}$ knockin strain (Guerra et al., 2003) with bitransgenic *Elas*-tTA/*tetO*-Cre mice that express the Cre recombinase under the control of the *Elastase* promoter in a tet-off system (P.J.G. and E.P.S., unpublished data). To verify the pattern of Cre expression in these mice, we crossed them with the Rosa26R reporter strain (Soriano, 1999). In the absence of doxycycline, *Elas*-tTA/*tetO*-Cre/Rosa26R embryos displayed β-galactosidase activity exclusively in pancreatic acinar cells, starting at embryonic day 16.5 (E16.5) (data not shown). Adult *Elas*-tTA/*tetO*-Cre/Rosa26R mice showed robust β-galactosidase activity in 20%–30% of acinar cells (Figure 1A). Some centroacinar cells also turned blue in the presence of X-gal (Figure 1B). However, due to the low number of these cells, we did not carry out precise quantitative analysis. More importantly, no β-galactosidase activity was detected in endocrine islets or in ductal cells of intra- and interlobular ducts (Figure 1A and Figure S1 in the Supplemental Data available with this article online). As a control, we did not observe detectable β-galactosidase activity in pancreata of adult animals continuously fed with doxycycline (data not shown).

The K-*Ras*^{LSLG12Vgeo} allele carries an IRES-*geo* cassette knocked in within its 3′ nontranslated sequences (Guerra et al., 2003). *Geo* is a bacterial gene that contains sequences from LacZ (the gene encoding β-galactosidase) and neo^{R} (the gene that confers resistance to neomycin) (Mountford et al., 1994). The internal ribosomal entry site (IRES) sequences placed 5′ of *geo* allow bicistronic expression of the chimeric Geo protein and the K-Ras^{G12V} oncoprotein upon Cre-dependent cleavage of the floxed STOP transcriptional cassette (Figure S2) (Guerra et al., 2003). This strategy allows identification of K-Ras^{G12V}-expressing cells by staining for β-galactosidase activity provided by the Geo protein.

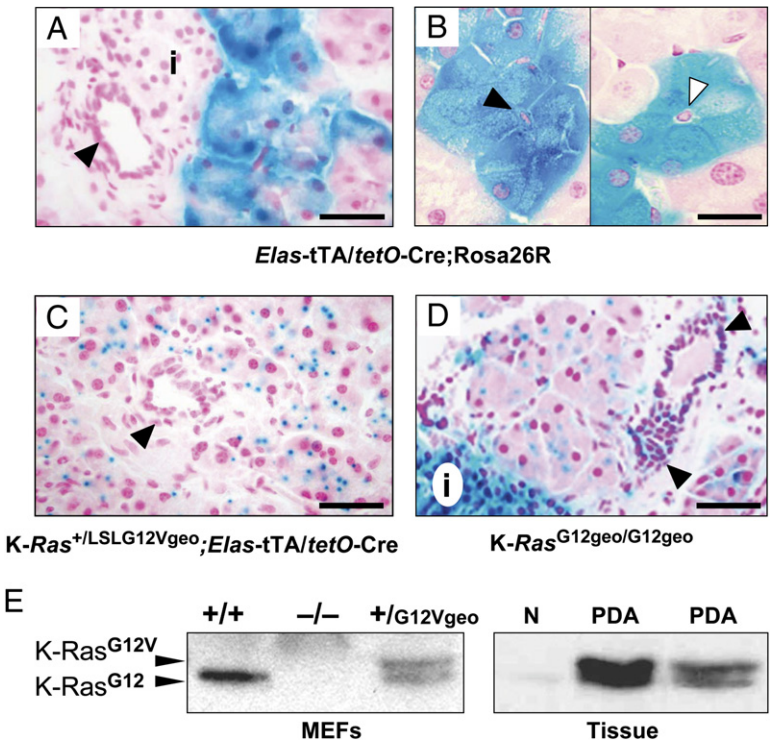

Figure 1. Analysis of K-Ras^{G12V} Expression

(A and B) β-galactosidase activity as a surrogate marker for Cre recombinase activity in *Elas*-tTA/*tetO*-Cre/Rosa26R mice. X-gal-stained cryostat sections of adult pancreata illustrate a patchy pattern of β-galactosidase activity (blue color) that results from Cre-mediated recombination of the Rosa26 locus. (A) X-gal staining is restricted to acinar and centroacinar cells. Note negative X-gal staining in ducts (arrowhead) and islet (i) (scale bar, 20 μm). (B) Higher magnification of centroacinar cells positive (black arrowhead) and negative (white arrowhead) for β-galactosidase activity (scale bar, 40 μm).

(C) β-galactosidase activity as a surrogate marker for expression of the K-Ras^{G12V} oncoprotein in K-*Ras*$^{+/LSLG12Vgeo}$/*Elas*-tTA/*tetO*-Cre mice. X-gal-stained cryostat section of adult pancreata of K-*Ras*$^{+/LSLG12Vgeo}$/*Elas*-tTA/*tetO*-Cre mice not exposed to doxycycline. X-gal staining is restricted to acinar cells. An intralobular duct (arrowhead) is not stained (scale bar, 20 μm).

(D) β-galactosidase activity as a surrogate marker for the expression of wild-type K-Ras^{G12} protein in K-*Ras*$^{G12geo/G12geo}$ mice. Note positive X-gal staining in acinar cells as well as in ductal (arrowheads) and endocrine (i) cells (scale bar, 20 μm).

(E) Western blot analysis of the expression levels of wild-type K-Ras^{G12} and oncogenic K-Ras^{G12V} proteins in MEFs of the indicated genotype as well as in normal (N) and tumor (PDA) pancreatic tissue obtained from K-*Ras*$^{+/LSLG12Vgeo}$/*Elas*-tTA/*tetO*-Cre mice. Migration of the K-Ras proteins is indicated by arrowheads.

Sections derived from K-*Ras*$^{+/LSLG12Vgeo}$;*Elas*-tTA/*tetO*-Cre mice displayed a spotted pattern of β-galactosidase staining instead of the uniform staining observed in pancreata of *Elas*-tTA/*tetO*-Cre/Rosa26R mice (Figure 1). The reasons for this differential pattern are unknown to us. However, the percentage of β-galactosidase-positive acinar and centroacinar cells was similar in both strains, indicating that the *Elastase* promotor-driven Cre recombinase cleaved the K-*Ras*^{LSLG12Vgeo} and Rosa26 alleles with similar efficiencies. As indicated above for *Elas*-tTA/*tetO*-Cre/Rosa26R mice, we did not observe any staining in ductal and endocrine cells present in sections obtained from either embryonic or adult K-*Ras*$^{+/LSLG12Vgeo}$;*Elas*-tTA/*tetO*-Cre animals (Figure 1C). However, these pancreatic cell types displayed β-galactosidase staining in sections obtained from control K-*Ras*$^{G12geo/G12geo}$ mice (C.G., A.J.S., M.C., P.D., and M.B., unpublished data), a strain that constitutively expresses the Geo protein from the endogenous K-*Ras* promoter (Figure 1D) (Figure S2).

Finally, we verified that bicistronic expression of Geo did not affect expression of the K-Ras^{G12V} oncoprotein in mouse embryonic fibroblasts (MEFs) or in pancreatic tissue. To this end, we separated normal K-Ras^{G12} and oncogenic K-Ras^{G12V} proteins by taking advantage of their differential mobility in SDS polyacrylamide gels (see Experimental Procedures) and determined their relative expression levels by western blotting with anti-K-Ras antibodies. As illustrated in Figure 1E, both K-*Ras*$^{+/G12Vgeo}$ MEFs and PDAs obtained from K-*Ras*$^{+/LSLG12Vgeo}$;*Elas*-tTA/*tetO*-Cre mice displayed a doublet in which both bands had the same intensity. Interestingly, the levels of expression of both K-*Ras* alleles, K-*Ras*$^{+}$ and K-*Ras*^{G12Vgeo}, were significantly increased in tumor tissue (see below).

Selective Expression of K-*Ras*^{G12V} in Cells of Acinar/Centroacinar Lineages Induces PanINs and Invasive PDA

Untreated K-*Ras*$^{+/LSLG12Vgeo}$;*Elas*-tTA/*tetO*-Cre mice in which expression of their K-*Ras*^{G12V} oncogenic allele is turned on during late embryonic development in acinar and possibly centroacinar cells developed focal morphological lesions between 1 and 3 months of age. These lesions were characterized as acinar-to-ductal metaplasia according to the criteria described in a recent consensus pathology report (Figure S3) (Hruban et al., 2006). This report summarizes the basic criteria of the main pancreatic lesions observed in a number of pancreatic models, including the one described here, based on their similarities to those lesions known to occur in human patients. These acinar-to-ductal metaplasias (one to ten per pancreata) were only observed in mice carrying the targeted K-*Ras*^{LSLG12Vgeo} allele (Figure S3), were positive for

β-galactosidase staining (data not shown), and preceded the appearance of PanIN lesions (see below). In older animals, these acinar-to-ductal metaplasias were associated with PanIN lesions in about 20% of the cases. Whether these metaplastic lesions are precursors of PanINs is a controversial issue that has been recently discussed (Hruban et al., 2006).

K-*Ras*$^{+/LSLG12Vgeo}$;*Elas*-tTA/*tetO*-Cre mice developed PanIN lesions that met the criteria defined by Hruban et al. (2006). Focal low-grade PanINs (PanIN1A) were observed in most (8/11) 3-month-old K-*Ras*$^{+/LSLG12Vgeo}$;*Elas*-tTA/*tetO*-Cre mice (Figure 2A). At this time, some animals (2/11) already contained diffuse PanIN1A/B lesions (Figure 2B). Three months later, most mice (8/12) had developed multiple diffuse PanIN1A/B (average of five lesions per pancreas), including high-grade PanIN2/3 lesions (2/12) and PDA (2/12) in some animals. At 12 months of age, 80% of the mice contained multiple PanINs (average of 15 lesions per pancreas) that had progressed to high-grade PanIN2/3 lesions (average of nine per pancreas) (Figure 2C). These PanINs were surrounded by a stromal reaction characterized by collagen deposits and fibroblastic proliferation (data not shown). Occasionally, we observed papillary mucinous structures in big interlobular ducts. Serial analysis of adjacent sections revealed that these lesions represented intraductal extension from adjacent intralobular PanINs (Figure 2D; Figure S4). More importantly, about half of these mice developed at least one PDA per pancreas. As in human PDA, these tumors contained abundant desmoplastic stroma (Figure 2E) and occasionally infiltrated the intestinal wall (Figure 2F). Some of them had lymphovascular embols (Figure 2G), a predictor of metastatic behavior.

In K-*Ras*$^{+/LSLG12Vgeo}$;*Elas*-tTA/*tetO*-Cre mice of 6 months of age or older, we occasionally observed areas of acinar hyperplasia in pancreatic lobules that did not contain either ductal metaplasia or PanINs (Figure S3C). Whether these lesions undergo transdifferentiation into ductal-like lesions such as ductal metaplasia or PanINs is not known. Yet, they never progress to malignant acinar cell carcinomas, at least until 20 months of age (data not shown).

Finally, all PanIN and PDA cells displayed β-galactosidase activity indicating that these lesions arose from cells expressing the oncogenic K-*Ras*^{G12Vgeo} allele. β-galactosidase expression was also detected in unaffected acinar/centroacinar cells as well as in metaplastic ducts (data not shown). However, no staining was detected in normal ductal cells, even in those cases in which they were adjacent to the PanIN (Figure 2H). Interestingly, the levels of β-galactosidase activity increased with PanIN grade to reach the highest levels in PDA (Figures 2I and 2J). These results are in agreement with those obtained by western blot analysis (Figure 1E). Since we observed overexpression of both alleles (Figure 1E) in the absence of overt K-*Ras* gene amplification (unpublished data), the increased levels of β-galactosidase expression observed during tumor progression must be a consequence of increased transcriptional activity on the K-*Ras* locus.

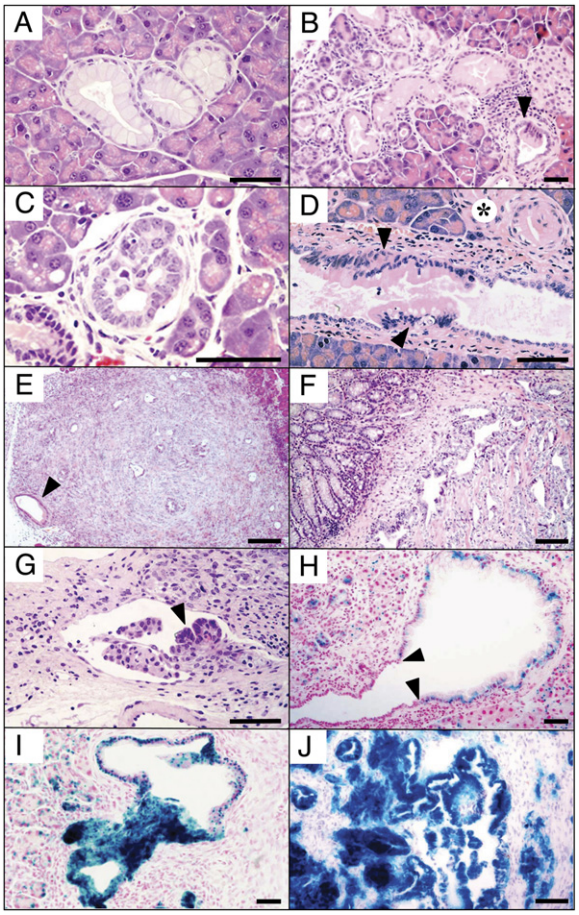

Figure 2. K-*Ras*$^{+/LSLG12Vgeo}$/*Elas*-tTA/*tetO*-Cre Mice Develop PanIN Lesions and Invasive PDA

(A) Focal PanIN1A characterized by columnar cells filled with mucin (H&E) (scale bar, 20 μm).

(B) Diffuse low-grade PanIN. Arrowhead shows a PanIN1B (H&E) (scale bar, 20 μm).

(C) Representative focal PanIN3 (H&E) (scale bar, 20 μm).

(D) Intralobular PanIN1A (asterisk) extending into an interlobular duct (arrowheads) (H&E) (scale bar, 20 μm).

(E) Poorly differentiated invasive PDA with desmoplastic stroma. PanINs are frequently found at the edges of the tumor (arrowhead) (H&E) (scale bar, 100 μm).

(F) Invasion of the intestinal wall by a PDA (H&E) (scale bar, 50 μm).

(G) Lymphovascular embol (arrowhead) in the peripancreatic fat tissue (H&E) (scale bar, 20 μm).

(H) β-galactosidase staining in a PanIN1A that extends into an interlobular duct. Note the sharp transition (arrowheads) between PanIN (stained) and ductal (unstained) cells (scale bar, 20 μm).

(I) β-galactosidase staining in PanIN2 lesion (scale bar, 20 μm).

(J) β-galactosidase staining in a PDA (scale bar, 50 μm).

Characterization of K-Ras^{G12V}-Induced PanINs

PanINs of K-*Ras*$^{+/LSLG12Vgeo}$;*Elas*-tTA/*tetO*-Cre mice have similar properties to those identified in human patients. They contained abundant mucin (Figure 3A) and immunostained for Cytokeratin 19 (Figure 3B), underscoring their ductal nature. PanINs often contained scattered endocrine cells (Figure 3C), a property also observed in human

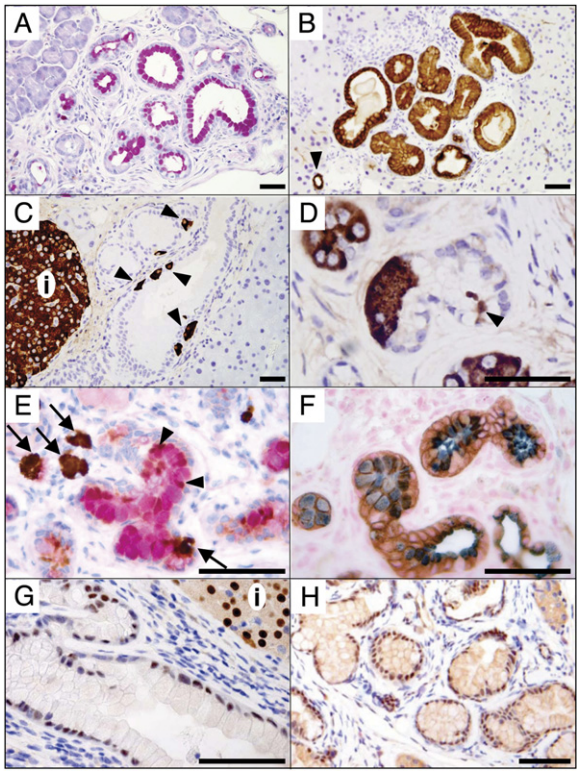

Figure 3. Histological Characterization of PanIN Lesions

(A) Mucin content of a diffuse PanIN1A revealed by diastase-PAS staining (scale bar, 20 μm).

(B) Cytokeratin 19 immunoreactivity in a diffuse PanIN1A and in a normal duct (arrowhead) (scale bar, 20 μm).

(C) Insulin immunostained cells within a PanIN1A (arrowheads) and an endocrine islet (i) (scale bar, 20 μm).

(D) Chymotrypsin expression in columnar cells (arrowhead) within a PanIN1A containing residual chymotrypsin-expressing acinar cells (scale bar, 20 μm).

(E) Low-grade PanIN lesion stained for diastase-PAS displaying cells immunoreactive for amylase (brown color, arrowheads). Neighboring acini stained for amylase are indicated by arrows (scale bar, 20 μm).

(F) Diffuse low-grade PanIN displaying both acinar (amylase, blue color) and ductal (cytokeratin 19, brown color) markers (scale bar, 20 μm).

(G) Diffuse PanIN1A showing nuclear Pdx1 immunostaining. Endocrine cells in an adjacent islet (i) serve as positive control (scale bar, 20 μm).

(H) Diffuse PanIN1A exhibiting nuclear Hes1 immunoreactivity (scale bar, 20 μm).

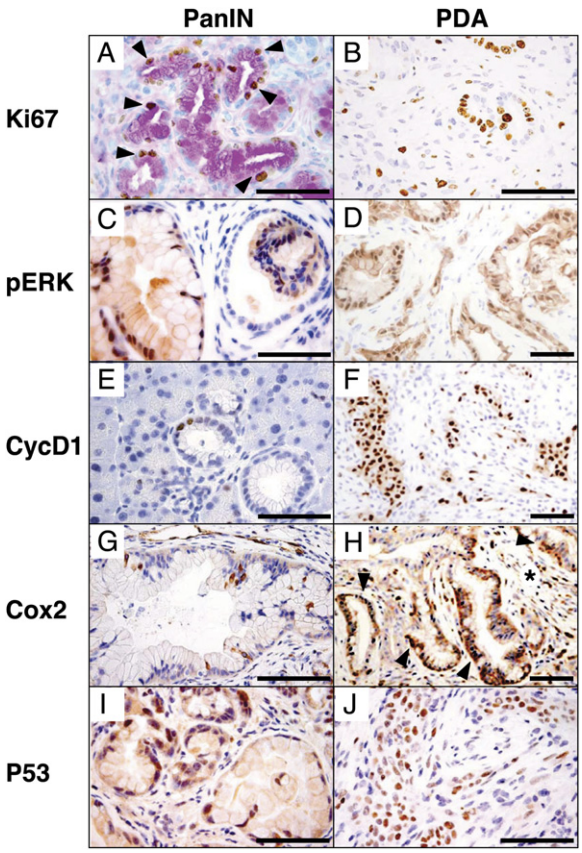

Figure 4. Signaling Pathways in PanINs and PDA

(A and B) Ki67 immunostaining (brown nuclei). The mucin content of the PanIN lesion (A) is highlighted by PAS staining. Arrowheads help to identify Ki67 positive cells (scale bars, 20 μm).

(C and D) Phospho-Erk immunostaining in PanIN1B and PDA (scale bars, 20 μm).

(E and F) Cyclin D1 immunostaining in PanIN1A and PDA (scale bars, 20 μm).

(G and H) Cyclooxygenase-2 immunoreactivity in PanIN1B and PDA (scale bars, 20 μm). In PDA, immunostaining is observed in tumor cells (arrowheads) and in the stroma (asterisk).

(I and J) P53 immunostaining in PanIN2 and PDA (scale bars, 20 μm).

lesions (Tezel et al., 2000). Occasionally, low-grade PanINs contained cells with acinar markers (Figures 3D and 3E). These structures may reflect a transient stage in PanIN formation in which some cells have not yet lost their acinar markers. In addition, some PanINs coexpressed both acinar and ductal markers, suggesting incomplete commitment to either lineage (Figure 3F). PanINs immunostained for Pdx1, an embryonic marker retained in adult endocrine islets but not in normal exocrine cells (Figure 3G) (Offield et al., 1996). Finally, these PanINs were also positive for Hes1, a marker for the Notch pathway also identified in human pancreatic tumors (Figure 3H) (Miyamoto et al., 2003).

Normal pancreatic cells showed low levels of Ki67 staining. The frequency of Ki67-positive cells remained low in low-grade PanINs to increase as they progressed to high-grade lesions (Figure 4A). PanINs also expressed a number of other proliferation-associated markers such as phospho-Erk (pERK) and Cyclin D1 (Figures 4C and 4E). In the case of Ki67 and Cyclin D1, positive cells appeared scattered within the PanIN. A similar pattern of expression was observed for cyclooxygenase-2 (Cox2) (Figure 4G). In contrast, pERK immunoreactivity appeared uniformly distributed throughout the PanIN (Figure 4C). Interestingly, pERK immunoreactivity could not be observed in normal ductal cells, even in ducts adjacent to PanIN lesions (Figure S5). In PDA, pERK was also found uniformly distributed in all tumoral but not stromal cells (Figure 4D). In addition, expression of Ki67, Cyclin D1, and Cox2 in

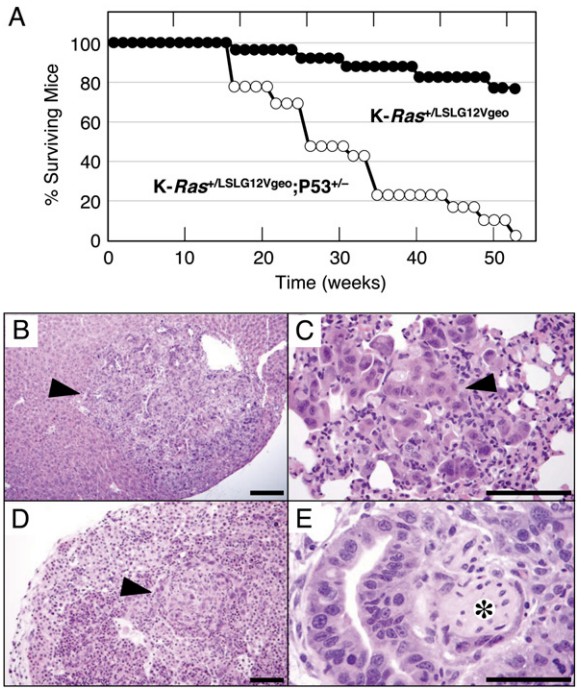

Figure 5. P53 Deficiency Cooperates with K-Ras^{G12V} to Induce Metastatic PDA

(A) Survival of K-*Ras*$^{+/LSLG12Vgeo}$;*Elas*-tTA/*tetO*-Cre (closed circles) and K-*Ras*$^{+/LSLG12Vgeo}$;*Elas*-tTA/*tetO*-Cre;P53$^{+/-}$ (open circles) mice.

(B–E) H&E-stained paraffin sections of (B) liver metastasis (arrowhead) (scale bar, 50 μm); (C) lung micrometastasis (arrowhead) (scale bar, 20 μm); (D) regional lymph node metastasis (arrowhead) (scale bar, 50 μm); and (E) perineural invasion (asterisk) (scale bar, 20 μm).

PDA was observed in a significantly higher percentage of cells (Figures 4B, 4F, and 4H). Finally, P53 nuclear staining, indicative of P53 inactivation (Bartek et al., 1991), was observed in some but not all high-grade PanINs, mostly PanIN3. Yet, PDAs were uniformly positive for P53 staining, indicating that P53 inactivation is a late event in the development of PDA (Figures 4I and 4J).

Loss of P53 Confers Metastatic Properties to K-Ras^{G12V}-Induced PDA

To assess the cooperation between K-*Ras*^{G12V} expression and P53 inactivation, a frequent mutation found in human PDA (Hruban et al., 2000), K-*Ras*$^{+/LSLG12Vgeo}$;*Elas*-tTA/*tetO*-Cre mice were crossed to *P53*$^{-/-}$ animals (Donehower et al., 1992). Half of the resulting K-*Ras*$^{+/LSLG12Vgeo}$;*Elas*-tTA/*tetO*-Cre;*P53*$^{+/-}$ mice died before 6 months of age, and none of them survived more than a year (Figure 5A). All mice (n = 17) developed moderately to poorly differentiated PDAs (often more than one per mouse) that invade surrounding tissues such as duodenum and stomach. Moreover, these animals presented peritoneal implants; perineural extension, a feature frequently found in human PDA; and metastases affecting liver, diaphragm, lung, lymph nodes, and spleen that are morphologically similar to their primary tumor (Figures 5B–5E).

Adult Pancreatic Cells Are Refractory to Transformation by the K-Ras^{G12V} Oncogene

Previous studies have indicated that widespread K-*Ras*^{G12V} expression in young mice efficiently induces lung adenomas and adenocarcinomas, but few pancreatic lesions (Guerra et al., 2003). Indeed, careful analysis of K-*Ras*$^{+/LSLG12Vgeo}$;RERT$^{ert/ert}$ mice treated for up to 12 weeks with 4-OHT only resulted in low-grade PanINs in a small percentage of animals in spite of widespread expression of the K-*Ras*^{G12Vgeo} allele in many cell types, including pancreatic acinar and ductal cells (C.G., A.J.S., M.C., P.D., and M.B., unpublished data). To examine whether postnatal pancreata might be more resistant to neoplastic development, we fed doxycycline to pregnant K-*Ras*$^{+/LSLG12Vgeo}$;*Elas*-tTA/*tetO*-Cre mice and their offspring until they were 10 days old (P10) to prevent expression of the K-*Ras*^{G12Vgeo} allele. Removal of doxycycline from the drinking water at P10 resulted in the expression of this allele as determined by β-galactosidase staining (Figure S6A). These K-*Ras*$^{+/LSLG12Vgeo}$;*Elas*-tTA/*tetO*-Cre mice developed PanIN lesions histologically indistinguishable from those described above, albeit with significantly increased latency. For instance, at 6 months of age, only one-third of the mice (4/12) displayed focal PanIN1A lesions. Likewise, at 12 months of age, only 37% of the mice (6/16) presented high-grade PanIN2/3 lesions, and only two of them (12%) had PDA.

Maintaining doxycycline in the drinking water for 2 months allowed us to turn on K-*Ras*^{G12Vgeo} expression in pancreata of adult mice (P60). Analysis of β-galactosidase activity revealed that K-*Ras*^{G12V} was expressed in about 20% of adult acinar cells, a percentage similar to that observed in mice not exposed to doxycycline (Figure S6B). Surprisingly, these mice did not develop obvious histological alterations in their pancreata, including acinar-to-ductal metaplasia and low-grade PanINs even when they were examined 6 (n = 8) or 12 (n = 3) months later. Moreover, their acinar cell compartment did not show significant differences in their proliferation rates when compared with control K-*Ras*$^{+/+}$;*Elas*-tTA/*tetO*-Cre littermates also exposed to doxycycline until P60 (data not shown). These observations indicate that expression of the K-*Ras*^{G12V} oncogene has few, if any, consequences for adult acinar cells, at least in the context of an otherwise normal pancreas (see below).

Chronic Pancreatitis Induces PanINs and PDA in Adult Mice Expressing the K-*Ras*^{G12V} Oncogene

In humans, one of the main risk factors for the development of PDA is chronic pancreatitis (Lowenfels et al., 1993; Malka et al., 2002). Therefore, we decided to interrogate whether chronic pancreatitis may cooperate with K-*Ras*^{G12Vgeo} expression in inducing PanIN lesions and PDA. To this end, P30 K-*Ras*$^{+/+}$;*Elas*-tTA/*tetO*-Cre (n = 12) and K-*Ras*$^{+/LSLG12Vgeo}$;*Elas*-tTA/*tetO*-Cre (n = 15) mice exposed to doxycycline since conception were chronically treated with low doses of caerulein (see Experimental Procedures). Caerulein is a cholecystokinin analog that induces secretion of pancreatic enzymes and,

depending on the dose and schedule used, can cause either acute or mild forms of pancreatitis (Willemer et al., 1992; Yoo et al., 2005). These caerulein-treated mice were continuously fed doxycycline for another month (until P60) to avoid recombination of the K-*Ras*^{LSLG12Vgeo} allele until the mice reached adulthood. Caerulein treatment did not affect the onset of K-*Ras*^{G12Vgeo} expression as determined by the absence of β-galactosidase staining in caerulein-treated P60 K-*Ras*$^{+/LSLG12Vgeo}$;*Elas*-tTA/*tetO*-Cre animals (data not shown).

One month after doxycycline withdrawal, P90 mice, regardless of genotype, displayed atrophic acini (about 20%) and mild panlobular lesions characteristic of chronic pancreatitis (Figures S7A and S7B). These atrophic acini had enlarged lumen and occasional focal cuboidal metaplasia. More importantly, histologically normal acini displayed a high proliferative index with 20%–30% of acinar cells positive for Ki67 staining versus less than 1% in untreated mice (Figures S7C and S7D). No such increase in Ki67 staining was observed in ductal or endocrine cells. Moreover, acini of caerulein-treated mice showed slightly increased levels of apoptosis (data not shown). In addition, pancreata derived from both cohorts of mice presented sparse inflammatory infiltrates.

At 5 months of age, the histological differences between K-*Ras*$^{+/LSLG12Vgeo}$;*Elas*-tTA/*tetO*-Cre and control mice became more evident. Pancreata of K-*Ras*^{G12Vgeo}-expressing mice displayed more severe acinar atrophy and increased fibrosis (Figure 6A). They also showed frequent acinar-to-ductal metaplasia as well as multifocal metaplastic ducts with atypical nuclear features and luminal budding suggestive of a premalignant behavior (Figure 6B). These lesions expressed Cytokeratin 19 and were only observed in the context of K-*Ras*^{G12Vgeo} expression and chronic pancreatitis. More importantly, half of these mice had already developed focal and diffuse low-grade PanIN lesions (data not shown).

At 8 months of age, the cohort expressing the oncogenic K-*Ras*^{G12V} allele (n = 6) displayed an exacerbated acinar atrophy with only 20% of their parenchyma corresponding to acinar cells as determined by chymotrypsin immunostaining as well as multifocal ductal atypia and severe fibrosis (Figure 6C). Caerulein-treated control K-*Ras*$^{+/+}$;*Elas*-tTA/*tetO*-Cre mice also displayed acinar atrophy but only in about half of their acinar parenchyma. More importantly, caerulein-treated K-*Ras*$^{+/LSLG12Vgeo}$;*Elas*-tTA/*tetO*-Cre animals had multiple PanIN lesions (an average of 33 per mouse), of which one-fifth were high-grade PanIN2/3. These lesions were often panlobular (Figure 6D) and extended into the big interlobular ducts (Figure 6E). Finally, one-third of the K-*Ras*^{G12V}-expressing mice had already developed invasive PDAs (Figure 6F). Similar results were observed 12 months after turning on K-*Ras*^{G12V} expression. No PanINs or PDA were observed in caerulein-treated control K-*Ras*$^{+/+}$;*Elas*-tTA/*tetO*-Cre mice (n = 4).

Chronic pancreatitis also served as a powerful tumor promoter in K-*Ras*$^{+/LSLG12Vgeo}$;*Elas*-tTA/*tetO*-Cre mice that expressed the K-*Ras*^{G12Vgeo} oncogenic allele during embryogenesis. Caerulein treatment of K-*Ras*$^{+/LSLG12Vgeo}$;*Elas*-tTA/*tetO*-Cre mice not exposed to doxycycline (n = 8) resulted in a significantly faster development of high-grade PanIN lesions and invasive PDA than in littermates not treated with caerulein. At 5 months of age, a time when only 15% of mice not suffering from chronic pancreatitis had developed high-grade PanINs, all caerulein-treated animals presented diffuse ductal metaplasia along with multiple high-grade PanINs (more than ten per mice). Moreover, half of the caerulein-treated mice had invasive PDA with desmoplastic stroma. At 8 months of age, all caerulein-treated K-*Ras*$^{+/LSLG12Vgeo}$;*Elas*-tTA/*tetO*-Cre mice had to be sacrificed due to the presence of multifocal in situ and invasive PDAs. A summary of the relative incidence of PanIN lesions and PDA observed in mice described throughout this study is provided in Figure 7.

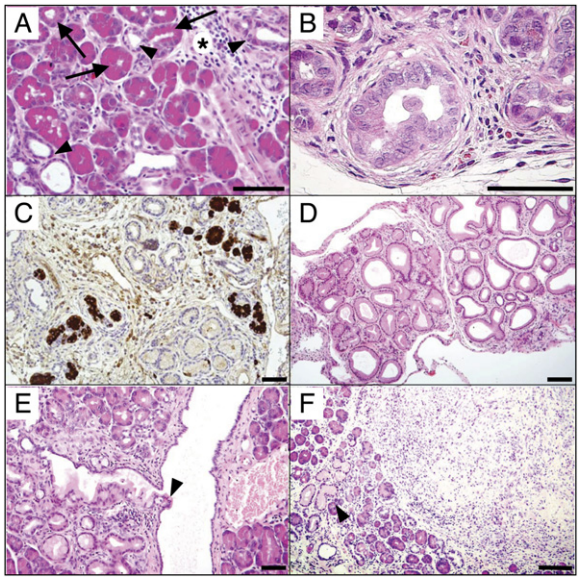

Figure 6. Chronic Pancreatitis Induces PanIN and PDA Lesions in K-*Ras*$^{+/LSLG12Vgeo}$;*Elas*-tTA/*tetO*-Cre, but Not in Control K-*Ras*$^{+/+}$;*Elas*-tTA/*tetO*-Cre Adult Mice

(A) Pancreata of a 3-month-old, caerulein-treated K-*Ras*$^{+/+}$;*Elas*-tTA/*tetO*-Cre mouse showing acinar atrophy with distended lumen and loss of apical granulations (arrows). Cuboidal metaplasia (arrowheads) and increased fibrosis with sparse inflammatory infiltrates (asterisk) are shown (H&E) (scale bar, 20 μm).

(B) Metaplastic ducts with atypical nuclear features and luminal budding in a 5-month-old, caerulein-treated K-*Ras*$^{+/LSLG12Vgeo}$;*Elas*-tTA/*tetO*-Cre mouse (H&E) (scale bar, 20 μm).

(C) Severe acinar atrophy attested by chymotrypsin immunostaining in an 8-month-old, caerulein-treated K-*Ras*$^{+/LSLG12Vgeo}$;*Elas*-tTA/*tetO*-Cre mouse (scale bar, 20 μm).

(D) Panlobular PanINs in an 8-month-old, caerulein-treated K-*Ras*$^{+/LSLG12Vgeo}$;*Elas*-tTA/*tetO*-Cre mouse (H&E) (scale bar, 20 μm).

(E) PanIN lesion extending into an interlobular duct (arrowhead) in an 8-month-old, caerulein-treated K-*Ras*$^{+/LSLG12Vgeo}$;*Elas*-tTA/*tetO*-Cre mouse (H&E) (scale bar, 20 μm).

(F) Poorly differentiated invasive PDA with desmoplastic stroma in an 8-month-old, caerulein-treated K-*Ras*$^{+/LSLG12Vgeo}$;*Elas*-tTA/*tetO*-Cre mouse. Low-grade PanIN lesions are present at the edge of the tumor (arrowhead) (H&E) (scale bar, 50 μm).

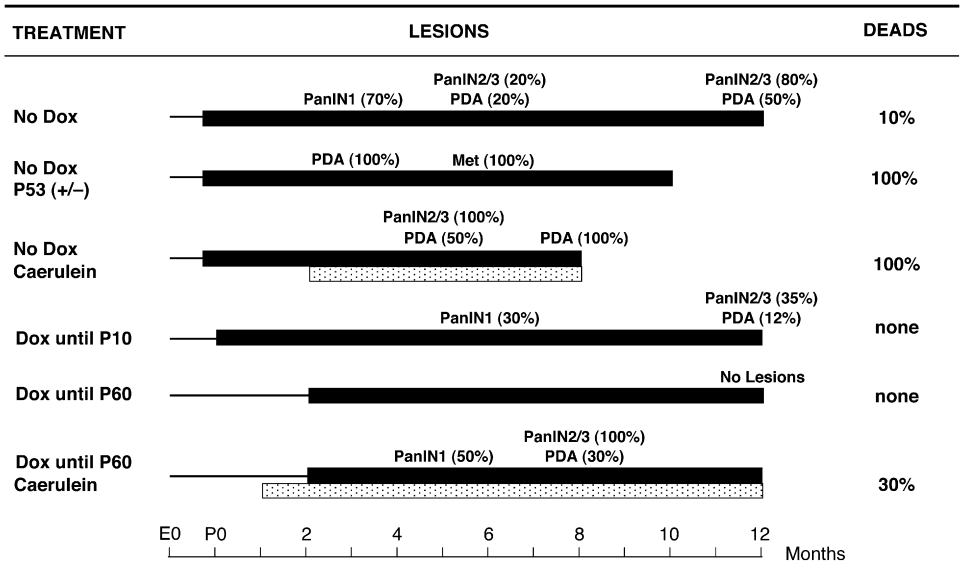

Figure 7. Summary of the Various Treatments Used in This Study

Thick boxes indicate the period of expression of the oncogenic K-*Ras*^{G12Vgeo} allele. Dotted boxes indicate caerulein treatment. The incidence of PanIN lesions and PDA at various times is indicated in parenthesis. Met, metastatic PDAs. The percentage of mice dead at 12 months of age is indicated in the right column.

Inflammatory Response

Caerulein-treated mice, regardless of genotype, developed innate and adaptive inflammatory responses. Two months after caerulein treatment, K-*Ras*$^{+/LSLG12Vgeo}$;*Elas*-tTA/*tetO*-Cre and control K-*Ras*$^{+/+}$;*Elas*-tTA/*tetO*-Cre mice displayed intra- and interlobular-mixed inflammatory infiltrates consisting of T cells (CD3^{+}) and macrophages (F4/80^{+}) associated with B cells (Pax5^{+}). The acute inflammatory component was attested by the presence of neutrophilic and eosinophilic granulocytes (Myeloperoxidase; MPO^{+}) Pancreata of 5-month-old mice presented a similar, albeit slightly increased pattern of inflammatory infiltrates, regardless of genotype. Finally, at 8 months of age, inflammatory infiltrates remain mostly chronic (Figure S8) and begin to accumulate plasma cell clusters (data not shown). K-*Ras*$^{+/LSLG12Vgeo}$;*Elas*-tTA/*tetO*-Cre mice, but not control littermates, showed active intralobular fibrosis that became most evident in animals of 5 months of age and older.

Linkage between inflammatory response and cancer is thought to be primarily mediated by activation of NF-κB transcription factors (Karin, 2006). NF-κB activation is often determined by its translocation to the nucleus (Karin and Ben-Neriah, 2000). Indeed, it has been previously reported that NF-κB becomes activated in caerulein-induced chronic pancreatitis (Steinle et al., 1999). In agreement with these observations, caerulein-induced pancreatitis resulted in strong NF-κB immunoreactivity in about 30%–40% of acinar cells in both K-*Ras*$^{+/LSLG12Vgeo}$;*Elas*-tTA/*tetO*-Cre (Figures 8A and 8B) and control K-*Ras*$^{+/+}$;*Elas*-tTA/*tetO*-Cre mice (data not shown). Levels of NF-κB expression in ductal and endocrine cells remained unaltered by caerulein treatment (Figures 8A and 8B). Most positive cells appeared in atrophic acini with loss of apical granulations and dilated lumen. Only a percentage of these acinar cells (5%–10%) showed immunoreactivity in their nuclei (Figures 8B and 8C). Whether these cells also expressed the oncogenic K-*Ras*^{G12Vgeo} allele remains to be determined. Yet, since control mice also show this pattern of NF-κB immunoreactivity, we cannot implicate NF-κB in PanIN formation. Indeed, low-grade PanINs did not express significant levels of NF-κB (Figure 8D). However, it is formally possible that turning on K-*Ras*^{G12Vgeo} expression in the context of NF-κB-positive cells contributes to malignant transformation. Finally, NF-κB immunostaining was observed in some high-grade lesions and in PDA (Figures 8E and 8F). However, this staining appeared to be mostly cytoplasmic (Figures 8E and 8F), thus suggesting that NF-κB does not play a role during progression to PDA.

DISCUSSION

To date, the only mouse model that has faithfully reproduced the progressive histological changes responsible for human PDA involves conditional activation of endogenous K-*Ras* oncogenes (Hingorani et al., 2003, 2005; Hruban et al., 2006). Expression of K-*Ras*^{G12D} in pancreatic precursors during early embryonic development induces the progressive development of PanINs histologically indistinguishable from those observed in patients with PDA (Hingorani et al., 2003, 2005; Aguirre et al., 2003). We have obtained similar results expressing an endogenous K-*Ras*^{G12V} oncogene (Guerra et al., 2003) in a more restricted pancreatic lineage limited to acinar

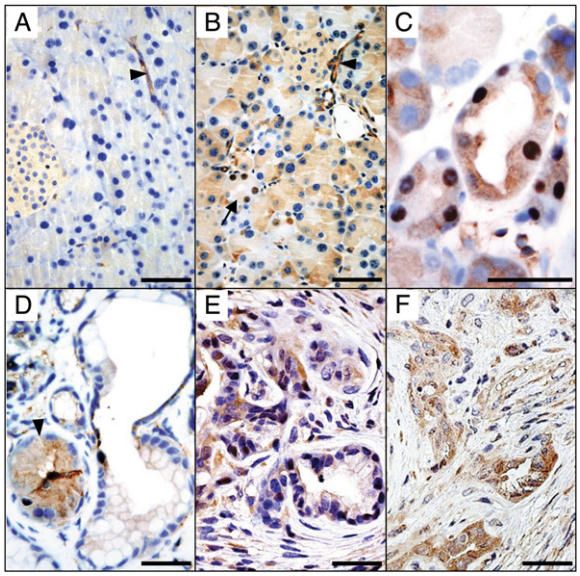

Figure 8. NF-κB Expression in Caerulein-Treated K-*Ras*$^{+/LSLG12Vgeo}$;*Elas*-tTA/*tetO*-Cre Mice

(A) NF-κB immunostaining in pancreata of an untreated 8-month-old mouse. Arrowhead shows strong NF-κB expression in normal ductal cells. Acinar and endocrine cells are unstained (scale bar, 20 μm).
(B) NF-κB expression in a littermate treated with caerulein. Few acinar cells display nuclear straining (arrow). Strong NF-κB expression in normal ductal cells is indicated by an arrowhead (scale bar, 20 μm).
(C) Higher magnification of distended atrophic acini showing cytoplasmic and/or nuclear-positive NF-κB immunostaining (scale bar, 20 μm).
(D) Lack of NF-κB expression in a PanIN1A lesion. A neighboring acinus shows cytoplasmic NF-κB immunoreactivity (arrowhead) (scale bar, 20 μm).
(E) NF-κB immunoreactivity in a high-grade PanIN (scale bar, 20 μm).
(F) NF-κB immunoreactivity in a PDA (scale bar, 20 μm).

and possibly centroacinar cells. Our observations strongly support the concept that PanINs and PDA result from differentiation of acinar (or possibly centroacinar) cells into ductal-like cells as a result of K-*Ras* oncogene expression.

Restricted expression of the endogenous K-*Ras*^{G12V} oncogene to acinar/centroacinar lineages also results in a highly metastatic phenotype when combined with loss of the P53 tumor suppressor. Thus, tumors derived from acinar/centroacinar cells or their precursors can also acquire the full spectrum of metastatic properties characteristic of human PDA. Cooperation of K-*Ras* oncogene expression in various settings with additional mutations, including deletion or inactivation of P53, Ink4a/Arf, Smad4, TGFβR2, or Smad4, as well as activation of Hedgehog signaling, also results in a significant acceleration of tumor development and, in some instances, acquisition of metastatic properties (Aguirre et al., 2003; Bardeesy et al., 2006; Hingorani et al., 2005; Ijichi et al., 2006; Pasca di Magliano et al., 2006).

The use of a tet-off strategy to express a Cre recombinase has allowed us to control the temporal expression of the targeted K-*Ras*^{G12V} oncogene at any time from embryonic development (E16.5) to adulthood by simply removing doxycycline from the drinking water of these animals. Doxycycline removal allows expression of the *Elastase*-driven Cre recombinase, which converts the silent K-*Ras*^{LSLG12Vgeo} allele into the transcriptionally active K-*Ras*^{G12Vgeo} allele. This strategy has made it possible to evaluate the effect of K-*Ras* oncogenes during postnatal development. Interestingly, turning on K-*Ras*^{G12V} expression in pancreata of young (P10) mice significantly reduces the incidence of PanINs, especially those of high grade. In addition, it also decreases the occurrence of PDA. More importantly, when K-*Ras*^{G12V} expression is delayed until adulthood, neither PanINs nor PDA is induced. These results are not due to decreased numbers of acinar cells expressing the K-*Ras*^{G12Vgeo} allele since the number of K-*Ras*^{G12Vgeo}-expressing cells in adult pancreata appears to be independent of the timing at which Cre activates expression of the silent K-*Ras*^{LSLG12Vgeo} allele. If PanINs and PDA originate by misdifferentiation of acinar (and/or centroacinar) progenitors, our results would suggest that the resistance of adult mice to K-*Ras*-induced PDA is a consequence of limited numbers of acinar/centroacinar progenitors in the adult pancreas. Alternatively, if PanINs and PDA PanINs arise by transdifferentiation of acinar (and/or centroacinar) cells, our results would suggest that adult acinar cells are less prone to transdifferentiate than those of embryonic (E16.5) or postnatal (P10) animals.

Adult mice became permissive to K-*Ras*^{G12V}-induced PanINs and PDA if they suffered a mild form of chronic pancreatitis. PanIN formation is completely dependent on K-*Ras*^{G12Vgeo} expression and follows a defined progression from low- to high-grade lesions that ends up in the appearance of invasive PDA. These observations indicate that chronic pancreatitis allows recapitulation in adult mice of the multistep transformation process observed when K-*Ras* oncogenes are expressed during embryonic development. A possible explanation for these observations is that pancreatitis increases the pool of K-Ras^{G12V}-susceptible cells, most likely acinar precursors. Additional support for this hypothesis is provided by the strong tumor-promoting effect that chronic pancreatitis exerts in K-*Ras*$^{+/LSLG12Vgeo}$;*Elas*-tTA/*tetO*-Cre mice that express K-*Ras*^{G12Vgeo} in embryonic precursors. However, we cannot rule out the possibility that pancreatitis may induce and/or facilitate transdifferentiation of mature acinar cells, making them susceptible to transformation by K-*Ras* oncogenes.

These observations may have important implications regarding the ontogeny of human PDA. The timing at which K-*Ras* mutations presumably initiate PDA in humans is not known (Kern, 2000; Kimura et al., 1998). Yet, it is unlikely that K-*Ras* oncogenes are mutated during embryonic or early postnatal development since there are no reports of pediatric PDA. Epidemiological studies have established a firm link between chronic pancreatitis and a percentage of human PDA (Lowenfels et al., 1993; Malka et al., 2002; Whitcomb and Pogue-Geile, 2002). Thus, it is tempting to speculate that human PDA may also stem from a combination of somatic mutations, mainly involving K-*Ras* oncogenes and nongenetic insults such as mild or

even asymptomatic events of pancreatitis, that may result in temporary tissue damage.

As observed in human patients, experimentally induced chronic pancreatitis results in acinar atrophy accompanied by increased proliferation of acinar cells, which is most likely a compensatory response. In addition, caerulein treatment induces innate and adaptive inflammatory responses characterized by invasion of macrophages and lymphocytes, respectively. These immune cells are also likely to induce cell proliferation by releasing inflammatory cytokines. This proliferative response may either amplify a pool of acinar progenitors susceptible to transformation by K-*Ras* oncogenes and/or facilitate transdifferentiation of mature acinar cells. However, our studies cannot discern which one of these proliferative stimuli contributes (and, if so, to what extent) to the generation of K-*Ras* oncogene-induced PanINs.

Previous studies have shown that caerulein treatment induces immediate nuclear NF-κB activity in acinar cells well before the onset of cellular injury including activation of an immune response (Steinle et al., 1999). In our model, nuclear translocation of NF-κB preceded PanIN formation. Moreover, no NF-κB immunostaining could be observed in PanIN lesions. Yet, our results cannot exclude the possibility that NF-κB activity may facilitate K-Ras^{G12V}-induced transformation of acinar cells. However, it is unlikely that NF-κB plays a role during tumor progression as previously described in colitis-associated colon cancer (Greten et al., 2004), since NF-κB immunostaining in high-grade PanINs and PDA remains mostly located in the cytoplasm. Ablation of NF-κB activators, such as IKKβ (Maeda et al., 2005), and/or inhibition of the immune response by genetic or pharmacological means should help to ascertain what mechanisms (proliferation as a direct response to tissue damage versus an inflammatory response) make adult K-*Ras*$^{+/LSLG12Vgeo}$;*Elas*-tTA/*tetO*-Cre mice susceptible to PDA.

EXPERIMENTAL PROCEDURES

Mouse Strains

Compound K-*Ras*$^{+/LSLG12Vgeo}$;*Elas*-tTA/*tetO*-Cre mice were generated by crossing the K-*Ras*$^{+/LSLG12Vgeo}$ strain, previously designated as K-*ras*$^{+/V12}$ (Guerra et al., 2003), with two strains carrying the *Elastase*-tTA (P.J.G. and E.P.S., unpublished data) and the *tetO*-PhCMV-Cre (Saam and Gordon, 1999) transgenes, respectively. The *Elastase*-tTA strain was generated by fusing a 205 bp DNA fragment containing the rat *Elastase* promoter and enhancer regions (Ornitz et al., 1987) with sequences encoding the tTA transactivator and a 600 bp fragment derived from the 3′ UTR of the human growth hormone gene that provided the polydenylation signal (P.J.G. and E.P.S., unpublished data). These transgenes allow expression of the bacterial Cre recombinase in cells normally expressing the *Elastase* gene under the negative control of doxycycline (tet-off system) (Furth et al., 1994). Doxycycline (2 mg/ml, Sigma) was provided in the drinking water as a sucrose (5% w/v) solution to pregnant mothers from the time of conception and to their offspring until the time required to turn on K-Ras^{G12V} expression (P10 or P60). Cre-mediated recombination removes the transcriptional STOP cassette present in the K-*Ras*^{LSLG12Vgeo} allele to allow bicistronic expression of K-Ras^{G12V} and Geo proteins (Guerra et al., 2003). Geo is a chimeric protein containing bacterial β-galactosidase and neomycin resistance sequences (Mountford et al., 1994). Chronic pancreatitis was induced by treatment with caerulein (Sigma), a cholecystokinin analog (Willemer et al., 1992; Yoo et al., 2005). Caerulein was administered as a single daily intraperitoneal injection (0.1 ml of a 50 μg/ml solution in saline) 5 days per week during the duration of the study. These experiments were approved by the CNIO Ethical Committee and performed in accordance with the guidelines for Ethical Conduct in the Care and Use of Animals as stated in The International Guiding Principles for Biomedical Research Involving Animals, developed by the Council for International Organizations of Medical Sciences (CIOMS).

Histopathology and Immunohistochemistry

Specimens were fixed in 10% buffered formalin and embedded in paraffin. For histopathological analysis, pancreata were serially sectioned (3 μm) and every fifth section was stained with hematoxylin and eosin (H&E). Remaining sections were used for immunohistochemical studies with the primary antibodies indicated with their specifications in Table S1. Following incubation with the primary antibodies, positive cells were visualized using 3,3-diaminobenzidine tetrahydrochloride plus (DAB+) as a chromogen. Staining for mucin content was carried out by using diastase-PAS. X-gal staining of cryosections (10 μm) (2–4 hr for tissues of *Elas*-tTA/*tetO*-Cre/Rosa26R mice and pancreata of tumor-bearing K-*Ras*$^{+/LSLG12Vgeo}$;*Elas*-tTA/*tetO*-Cre animals and up to 48 hr for normal tissues of K-*Ras*$^{+/LSLG12Vgeo}$;*Elas*-tTA/*tetO*-Cre mice) was carried out as previously described (Guerra et al., 2003). Counterstaining was performed with nuclear fast red or hematoxylin.

Western Blot Analysis

Immunoprecipitates were obtained by incubating 500 μg (MEFs) or 1 mg (tissues) of cell extracts with the Y13-259 rat monoclonal antibody (Ab-1, Calbiochem), separated in 15% SDS-PAGE, transferred to nitrocellulose filters, and incubated with anti-K-Ras-specific polyclonal antibody F-234 (Santa Cruz Biotechnology). F-234 antibodies were detected with a polyclonal goat anti-mouse horseradish peroxidase-linked secondary antibody and visualized with enhanced chemioluminiscent system (ECL Plus, Amersham). Wild-type K-Ras^{G12} and oncogenic K-Ras^{G12V} proteins display different migration (Joyce et al., 1989).

Supplemental Data

The Supplemental Data include eight supplemental figures and one supplemental table and can be found with this article online at http://www.cancercell.org/cgi/content/full/11/3/291/DC1/.

ACKNOWLEDGMENTS

We thank M. Lamparero, M. San Román, and R. Villar for their excellent technical assistance. We also value the excellent support provided by V. Alvarez, L, Castaño, V. Coca, P. González, and C. Medina (Comparative Pathology Unit) and O. Dominguez (Genomic Unit) with histopathology and genotyping analysis, respectively. We thank J.I. Gordon for providing the *tet*O-PhCMV-Cre mice and C.V. Wright for the anti-Pdx1 antibody. This work was supported by grants from the Ministerio de Ciencia y Tecnología (SAF2003-05172), Ministerio de Educación y Ciencia (SAF2004-20477-E), European Commission (QLG2-CT-2002-00930 and LSHC-CT-2004-503438), Comunidad Autónoma de Madrid (GR/SAL/0587/2004), and Fundación Médica Mutua Madrileña to M.B.; Fondo de Investigación Sanitaria (PI042124), and Comunidad Autónoma de Madrid (GR/SAL/0349/2004) to C.G.; and INSERM and Association pour la Recherche contre le Cancer (Région Aquitaine) to P.D., A.J.S., and L.V. are supported by fellowships from Formación de Profesorado Universitario (FPU, Ministerio de Educación y Ciencia) and Fundación Ramón Areces, respectively. The CNIO is partially supported by the RTICCC (Red de Centros de Cáncer; FIS C03/10).

Received: September 22, 2006
Revised: November 28, 2006
Accepted: January 11, 2007
Published: March 12, 2007

REFERENCES

Aguirre, A.J., Bardeesy, N., Sinha, M., Lopez, L., Tuveson, D.A., Horner, J., Redston, M.S., and DePinho, R.A. (2003). Activated Kras and Ink4a/Arf deficiency cooperate to produce metastatic pancreatic ductal adenocarcinoma. Genes Dev. *17*, 3112–3126.

Almoguera, C., Shibata, D., Forrester, K., Martin, J., Arnheim, N., and Perucho, M. (1988). Most human carcinomas of the exocrine pancreas contain mutant c-K-ras genes. Cell *53*, 549–554.

Bardeesy, N., Cheng, K.H., Berger, J.H., Chu, G.C., Pahler, J., Olson, P., Hezel, A.F., Horner, J., Lauwers, G.Y., Hanahan, D., and Depinho, R.A. (2006). Smad4 is dispensable for normal pancreas development yet critical in progression and tumor biology of pancreas cancer. Genes Dev. *20*, 3130–3146.

Bartek, T., Bartkova, J., Vojtesek, B., Staskova, Z., Lukas, J., Rejthar, A., Kovarik, J., Midley, C.A., Gannon, J.V., and Lane, D. (1991). Aberrant expression of the p53 oncoprotein is a common feature of a wide spectrum of human malignancies. Oncogene *6*, 1699–1703.

Brembeck, F.H., Schreiber, F.S., Deramaudt, T.B., Craig, L., Rhoades, B., Swain, G., Grippo, P., Stoffers, D.A., Silberg, D.G., and Rustgi, A.K. (2003). The mutant K-ras oncogene causes pancreatic periductal lymphocytic infiltration and gastric mucous neck cell hyperplasia in transgenic mice. Cancer Res. *63*, 2005–2009.

Donehower, L.A., Harvey, M., Slagle, B.L., McArthur, M.J., Montgomery, C.A., Butel, J.S., and Bradley, A. (1992). Mice deficient for p53 are developmentally normal but susceptible to spontaneous tumours. Nature *356*, 215–221.

Furth, P.A., St Onge, L., Boger, H., Gruss, P., Gossen, M., Kistner, A., Bujard, H., and Hennighausen, L. (1994). Temporal control of gene expression in transgenic mice by a tetracycline-responsive promoter. Proc. Natl. Acad. Sci. USA *91*, 9302–9306.

Greten, F.R., Eckmann, L., Greten, T.F., Park, J.M., Li, Z.W., Egan, L.J., Kagnoff, M.F., and Karin, M. (2004). IKKbeta links inflammation and tumorigenesis in a mouse model of colitis-associated cancer. Cell *118*, 285–296.

Grippo, P.J., Nowlin, P.S., Demeure, M.J., Longnecker, D.S., and Sandgren, E.P. (2003). Preinvasive pancreatic neoplasia of ductal phenotype induced by acinar cell targeting of mutant Kras in transgenic mice. Cancer Res. *63*, 2016–2019.

Guerra, C., Mijimolle, N., Dhawahir, A., Dubus, P., Barradas, M., Serrano, M., Campuzano, V., and Barbacid, M. (2003). Tumor induction by an endogenous K-ras oncogene is highly dependent on cellular context. Cancer Cell *4*, 111–120.

Hingorani, S.R., Petricoin, E.F., Maitra, A., Rajapakse, V., King, C., Jacobetz, M.A., Ross, S., Conrads, T.P., Veenstra, T.D., Hitt, B.A., et al. (2003). Preinvasive and invasive ductal pancreatic cancer and its early detection in the mouse. Cancer Cell *4*, 437–450.

Hingorani, S.R., Wang, L., Multani, A.S., Combs, C., Deramaudt, T.B., Hruban, R.H., Rustgi, A.K., Chang, S., and Tuveson, D.A. (2005). Trp53R172H and KrasG12D cooperate to promote chromosomal instability and widely metastatic pancreatic ductal adenocarcinoma in mice. Cancer Cell *7*, 469–483.

Hruban, R.H., Wilentz, R.E., and Kern, S.E. (2000). Genetic progression in the pancreatic ducts. Am. J. Pathol. *156*, 1821–1825.

Hruban, R.H., Wilentz, R.E., and Maitra, A. (2005). Identification and analysis of precursors to invasive pancreatic cancer. Methods Mol. Med. *103*, 1–13.

Hruban, R.H., Adsay, N.V., Albores-Saavedra, J., Anver, M.R., Biankin, A.V., Boivin, G.P., Furth, E.E., Furukawa, T., Klein, A., Klimstra, D.S., et al. (2006). Pathology of genetically engineered mouse models of pancreatic exocrine cancer: consensus report and recommendations. Cancer Res. *66*, 95–106.

Ijichi, H., Chytil, A., Gorska, A.E., Aakre, M.E., Fujitani, Y., Fujitani, S., Wright, C.V., and Moses, H.L. (2006). Aggressive pancreatic ductal adenocarcinoma in mice caused by pancreas-specific blockade of transforming growth factor-beta signaling in cooperation with active Kras expression. Genes Dev. *20*, 3147–3160.

Jackson, E.L., Willis, N., Mercer, K., Bronson, R.T., Crowley, D., Montoya, R., Jacks, T., and Tuveson, D.A. (2001). Analysis of lung tumor initiation and progression using conditional expression of oncogenic K-ras. Genes Dev. *15*, 3243–3248.

Joyce, A.D., D'Emilia, J.C., Steele, G., Jr., Libertino, J.A., Silverman, M.L., and Summerhayes, I.C. (1989). Detection of altered H-ras proteins in human tumors using western blot analysis. Lab. Invest. *61*, 212–218.

Karin, M. (2006). Nuclear factor-kappaB in cancer development and progression. Nature *441*, 431–436.

Karin, M., and Ben-Neriah, Y. (2000). Phosphorylation meets ubiquitination: the control of NF-[kappa]B activity. Annu. Rev. Immunol. *18*, 621–663.

Kawaguchi, Y., Cooper, B., Gannon, M., Ray, M., MacDonald, R.J., and Wright, C.V. (2002). The role of the transcriptional regulator Ptf1a in converting intestinal to pancreatic progenitors. Nat. Genet. *32*, 128–134.

Kern, S.E. (2000). Molecular genetic alterations in ductal pancreatic adenocarcinomas. Med. Clin. North Am. *84*, 691–695.

Kim, S.K., and MacDonald, R.J. (2002). Signaling and transcriptional control of pancreatic organogenesis. Curr. Opin. Genet. Dev. *12*, 540–547.

Kimura, W., Morikane, K., Esaki, Y., Chung, W.C., and Pour, P.M. (1998). Histologic and biologic patterns of microscopic pancreatic ductal adenocarcinomas detected incidentally at autopsy. Cancer *82*, 1839–1849.

Lowenfels, A.B., Maisonneuve, P., Cavallini, G., Ammann, R.W., Lankisch, P.G., Andersen, J.R., Dimagno, E.P., Andren-Sandberg, A., and Domellof, L. (1993). Pancreatitis and the risk of pancreatic cancer. International Pancreatitis Study Group. N. Engl. J. Med. *328*, 1433–1437.

Maeda, S., Kamata, H., Luo, J.L., Leffert, H., and Karin, M. (2005). IKKbeta couples hepatocyte death to cytokine-driven compensatory proliferation that promotes chemical hepatocarcinogenesis. Cell *121*, 977–990.

Maitra, A., Fukushima, N., Takaori, K., and Hruban, R.H. (2005). Precursors to invasive pancreatic cancer. Adv. Anat. Pathol. *12*, 81–91.

Malka, D., Hammel, P., Maire, F., Rufat, P., Madeira, I., Pessione, F., Levy, P., and Ruszniewski, P. (2002). Risk of pancreatic adenocarcinoma in chronic pancreatitis. Gut *51*, 849–852.

Miyamoto, Y., Maitra, A., Ghosh, B., Zechner, U., Argani, P., Iacobuzio-Donahue, C.A., Sriuranpong, V., Iso, T., Meszoely, I.M., Wolfe, M.S., et al. (2003). Notch mediates TGF alpha-induced changes in epithelial differentiation during pancreatic tumorigenesis. Cancer Cell *3*, 565–576.

Mountford, P., Zevnik, B., Duwel, A., Nichols, J., Li, M., Dani, C., Robertson, M., Chambers, I., and Smith, A. (1994). Dicistronic targeting constructs: reporters and modifiers of mammalian gene expression. Proc. Natl. Acad. Sci. USA *91*, 4303–4307.

Offield, M.F., Jetton, T.L., Labosky, P.A., Ray, M., Stein, R.W., Magnuson, M.A., Hogan, B.L., and Wright, C.V. (1996). PDX-1 is required for pancreatic outgrowth and differentiation of the rostral duodenum. Development *122*, 983–995.

Ornitz, D.M., Hammer, R.E., Davison, B.L., Brinster, R.L., and Palmiter, R.D. (1987). Promoter and enhancer elements from the rat elastase I gene function independently of each other and of heterologous enhancers. Mol. Cell. Biol. *7*, 3466–3472.

Pasca di Magliano, M., Sekine, S., Ermilov, A., Ferris, J., Dlugosz, A.A., and Hebrok, M. (2006). Hedgehog/Ras interactions regulate early stages of pancreatic cancer. Genes Dev. *20*, 3161–3173.

Quaife, C.J., Pinkert, C.A., Ornitz, D.M., Palmiter, R.D., and Brinster, R.L. (1987). Pancreatic neoplasia induced by ras expression in acinar cells of transgenic mice. Cell *48*, 1023–1034.

Saam, J.R., and Gordon, J.I. (1999). Inducible Gene Knockouts in the Small Intestinal and Colonic Epithelium. J. Biol. Chem. *274*, 38071–38082.

Soriano, P. (1999). Generalized lacZ expression with the ROSA26 Cre reporter strain. Nat. Genet. *21*, 70–71.

Stanger, B.Z., Stiles, B., Lauwers, G.Y., Bardeesy, N., Mendoza, M., Wang, Y., Greenwood, A., Cheng, K.H., McLaughlin, M., Brown, D., et al. (2005). Pten constrains centroacinar cell expansion and malignant transformation in the pancreas. Cancer Cell *8*, 185–195.

Steinle, A.U., Weidenbach, H., Wagner, M., Adler, G., and Schmid, R.M. (1999). NF-κB/Rel Activation in cerulein pancreatitis. Gastroenterology *116*, 420–430.

Tezel, E., Nagasaka, T., Nomoto, S., Sugimoto, H., and Nakao, A. (2000). Neuroendocrine-like differentiation in patients with pancreatic carcinoma. Cancer *89*, 2230–2236.

Tuveson, D.A., and Hingorani, S.R. (2005). Ductal pancreatic cancer in humans and mice. Cold Spring Harb. Symp. Quant. Biol. *70*, 65–72.

Tuveson, D.A., Zhu, L., Gopinathan, A., Willis, N.A., Kachatrian, L., Grochow, R., Pin, C.L., Mitin, N.Y., Taparowsky, E.J., Gimotty, P.A., et al. (2006). Mist1-KrasG12D knock-in mice develop mixed differentiation metastatic exocrine pancreatic carcinoma and hepatocellular carcinoma. Cancer Res. *66*, 242–247.

Whitcomb, D.C., and Pogue-Geile, K. (2002). Pancreatitis as a risk for pancreatic cancer. Gastroenterol. Clin. North Am. *31*, 663–678.

Willemer, S., Elsasser, H.P., and Adler, G. (1992). Hormone-induced pancreatitis. Eur. Surg. Res. *24*, 29–39.

Yoo, B.M., Oh, T.Y., Kim, Y.B., Yeo, M., Lee, J.S., Surh, Y.J., Ahn, B.O., Kim, W.H., Sohn, S., Kim, J.H., et al. (2005). Novel antioxidant ameliorates the fibrosis and inflammation of cerulein-induced chronic pancreatitis in a mouse model. Pancreatol. *5*, 165–176.